Exploratory Testing of a Radio-Frequency Thruster for Small Satellites

IEPC-2017-425

Presented at the 35th International Electric Propulsion Conference
Georgia Institute of Technology • Atlanta, Georgia • USA
October 8 – 12, 2017

E. Kralkina[1] and I. Zadiriev[2]
Lomonosov Moscow State University, Moscow, 119991, Russia

A. Kharlan[3]
Avant – Space Systems Ltd., Moscow, 143026, Russia

Abstract: This paper discusses the process of developing an RF gridded ion thruster. Possible applications of the thruster are discussed and an analysis is conducted in order to determine the optimal parameters of a thruster. In the second part of the paper, an approach taken to the thruster design is discussed. A series of experiments were conducted in order to determine the optimal layout of the thruster required to satisfy the needs of possible space missions.

Nomenclature

Ci	=	ion cost calculated with RF power
*Ci**	=	ion cost calculated with power deposited into plasma
I	=	specific impulse
i_b	=	ion beam current
L	=	discharge chamber length
Mo	=	initial mass of the spacecraft
Mp	=	mass of the propellant used
Pgen	=	RF power
Ppl	=	power deposited into plasma
Rant	=	RF antenna resistance
Rpl	=	equivalent plasma resistance
Δv	=	delta-v required for maneuvers

I. Introduction

DURING the past stages of spaceflight development precise satellite positioning and station-keeping were mainly done with monopropellant or bipropellant chemical thrusters. One of its main disadvantages is their low specific impulse, which led to reduced lifetime and required storing excessive amounts of propellant onboard. However, at the same time, the lifetime of electronics was also limited due to low reliability and low radiation resistance, thus the reliability requirements at high mission lifetimes could not be met anyway. Nowadays, as there are electronics capable of operating in space for dozens of years and compact to the point where adding redundant computers is of no serious concern, the question of possible prolonging mission lifetimes reemerges. Thrusters developed now with high specific impulse are the way to meet these new requirements. However, among these

[1] Leading Researcher, Physical department, ekralkina@mail.ru.
[2] Researcher, Physical department, s_333_52@mail.ru.
[3] Lead engineer, a.kharlan@avantspace.com.

thrusters there are also various subtypes with thrusts, impulses, and power consumptions significantly different from each other.

For proper assessment of possible applications of a thruster in various space missions, a number of hypotheses was studied concerning the shape of the future missions that may require a thruster like the one being developed. These possible missions were modelled, and power, time and propellant consumption were studied for various orbital maneuvers these missions might perform. It was then concluded whether the missions might require specifically a high-impulse ion thruster. The first part of this paper describes the results of this analysis.

Gridded ion thruster have been being developed for more than 50 years now [1, 7]. They always contain such parts as discharge chamber, where the plasma is generated that becomes the source of ions; and ion-optical system for extracting and accelerating ions. The fact that these parts work independently is a distinguishing feature of gridded ion thrusters.

RIT-class thrusters originated from the University of Giessen in the 1960s [2] works on the principle of inductive RF discharge. An inductor (antenna) mounted on a surface of the discharge chamber ignites and maintains the discharge with relatively high plasma density and modest level of power coupling. Nowadays, to improve thrusters of this class it is suggested to use an RF discharge of lower frequencies [3]. This would decrease the capacitive component of the discharge significantly and make RF generator less complex.

Another approach, which is described in the second part of the present paper, is to use an external magnetic field allowing optimizing the power coupling to plasma and raising plasma density at given RF power values. To study feasibility of this approach, an attempt was made to analyze advantages and disadvantages of operational processes based on modified inductive RF discharge. In other words, this paper describes an attempt to answer a question about which layout is preferable for different conditions of thruster operation. In order to do this, thruster parameters of a thruster with a purely inductive RF discharge were compared to those of a thruster with external magnetic field applied.

II. Thruster Applications: Feasibility Assessment

A. Station-keeping

To evaluate orbital perturbations precise modelling of satellites' motion was conducted. Among all the perturbations, naturally, the atmospheric drag is the most significant.

It can be shown that a 12 mN thruster with 3500 sec specific impulse can be used for station-keeping (mainly for the semi-major axis) in small spacecraft with the mass up to 150 kg. This sort of spacecraft is now commonly used in remote sensing. A case was studied when a spacecraft is in a circular sun-synchronous orbit with an altitude of 500 km. A variation of the semi-major axis for this case is shown in Fig. 1.

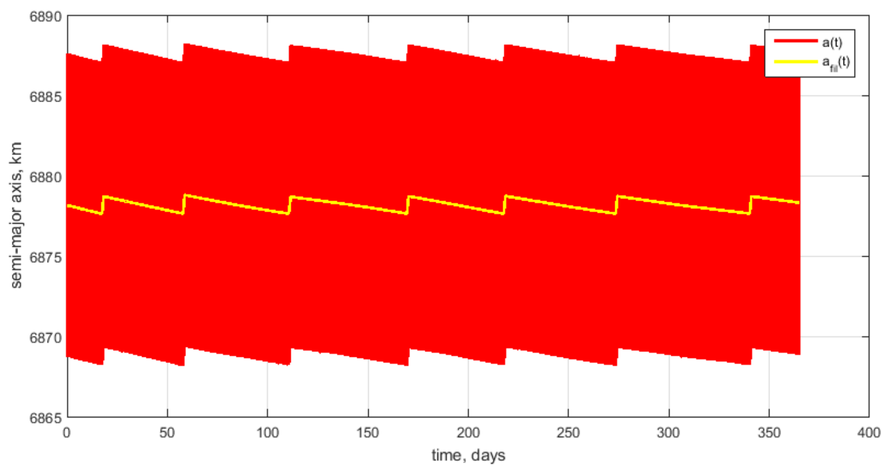

Figure 1. Orbit semi-major axis variation over a year.
Red line: actual value; yellow line: mean value. Each jump upwards (rather abrupt in this time scale) represents a station-keeping session.

The spacecraft mass is reduced as the propellant is used for each station-keeping session. This is illustrated in Fig. 2.

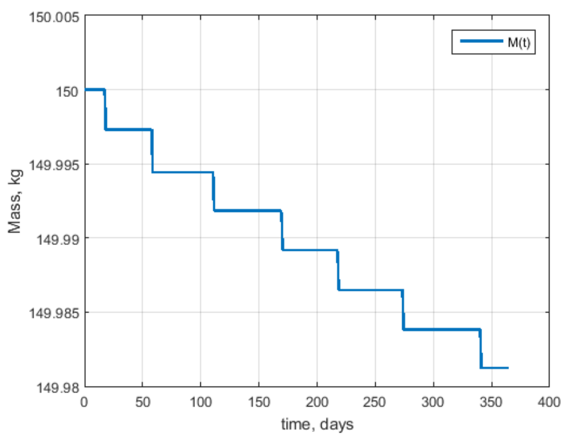

Figure 2. Spacecraft mass variation over a year.

Now, to estimate the delta-v used over one year, using Tsiolkovsky rocket equation (Eq.1):

$$\Delta v = I \cdot \ln \frac{M_0}{M_0 - M_P} = 4.12 \quad m/s \tag{1}$$

Now, say a hypothetical chemical thruster is used instead. The specific impulse of such a thruster can be about 100 sec (as has Low Power Resistojet produced by SSTL). Then, inverting the Eq.1 (Eq.2):

$$M_P = M_0 - \frac{M_0}{\exp(\frac{\Delta v}{I})} = 0.629 \quad kg \tag{2}$$

Figure 2 shows that the ion thruster used about 0.018 kg of propellant over the year. In case of such spacecraft it can help save up to 6 kg of mass over 10 years, and that is station-keeping only.

B. Deorbiting

As the global aerospace community becomes more and more concerned with the space debris problem, one can infer that in the nearest future it will be required by law to deorbit spacecraft after the end of its mission. Even today, many manufacturers of LEO satellites guarantee that their satellites will be deorbited in 10 to 15 years after the end of their missions.

The analysis done also shows the advantages an ion thruster has in comparison to a chemical thruster when a spacecraft is deorbited. These advantages are also mainly due to its high specific impulse. If a spacecraft is to be deorbited, the higher its orbit, the more is the need to use a thruster with a high specific impulse, consuming significantly less propellant. Using a low impulse for deorbiting thruster can require up to 15% of the spacecraft mass in propellant, which is not satisfactory.

If, say, a 150 kg spacecraft in a circular 800 km orbit is to be maneuvered to 500x800 km orbit to speed up the orbit decay, the ion thruster consumes only 338 g of propellant, whilst a hypothetical chemical thruster would use 11.37 kg. If the spacecraft is to re-enter immediately (meaning the perigee should dip into the atmosphere at 150-200 km), the chemical thruster would consume more than 21 kg.

C. Non-coplanar orbit phasing

The emerging of thrusters with very high specific impulse opens new possibilities in the area of non-coplanar orbit changes. It is applicable in the situations such as described in Ref. 4, where there is a possibility to launch many satellites in one launch, only not all of them are destined for the same RAAN. To avoid purchasing more launches it might be feasible to perform non-coplanar maneuvering instead. A possible constellation, such as described in Ref. 4 is illustrated in Fig. 3.

In this case, direct maneuvers to change RAAN are not optimal. Instead, the following strategy might be applied:

1. The launch vehicle delivers a cluster of satellites into the phasing orbit, with inclination and altitude slightly different from those of the target orbit;
2. First group of satellites, which is meant to be delivered into the first plane, jettisons from the cluster;
3. The detached group then begins a maneuver towards the target orbit (changing inclination);

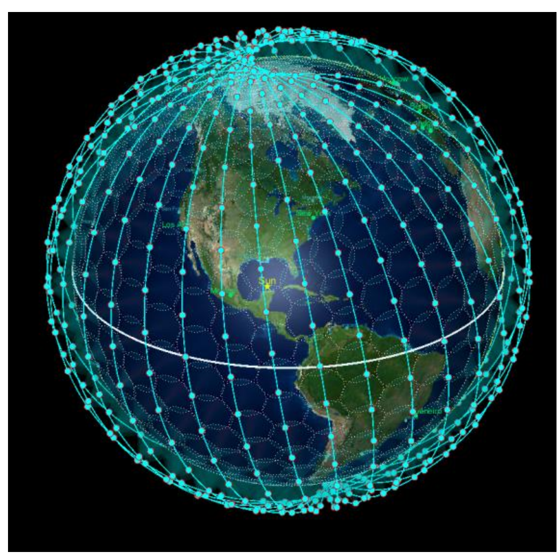

Figure 3. A constellation of 510 spacecraft.

4. The remaining satellites fly passively until the RAAN secular drift brings them to the desired position, where they perform the same maneuver operations;
5. After reaching the target orbit, each satellite changes its semi-major axis so that perigee altitude remains equal to the radius of the operational orbit, and apogee altitude is slightly bigger than that. Thus, the difference in orbital periods cause the satellite's phase to lag, and therefore it is possible to deliver the satellite into its operational point (this is in-orbit phasing).

This strategy is illustrated in Fig. 4.

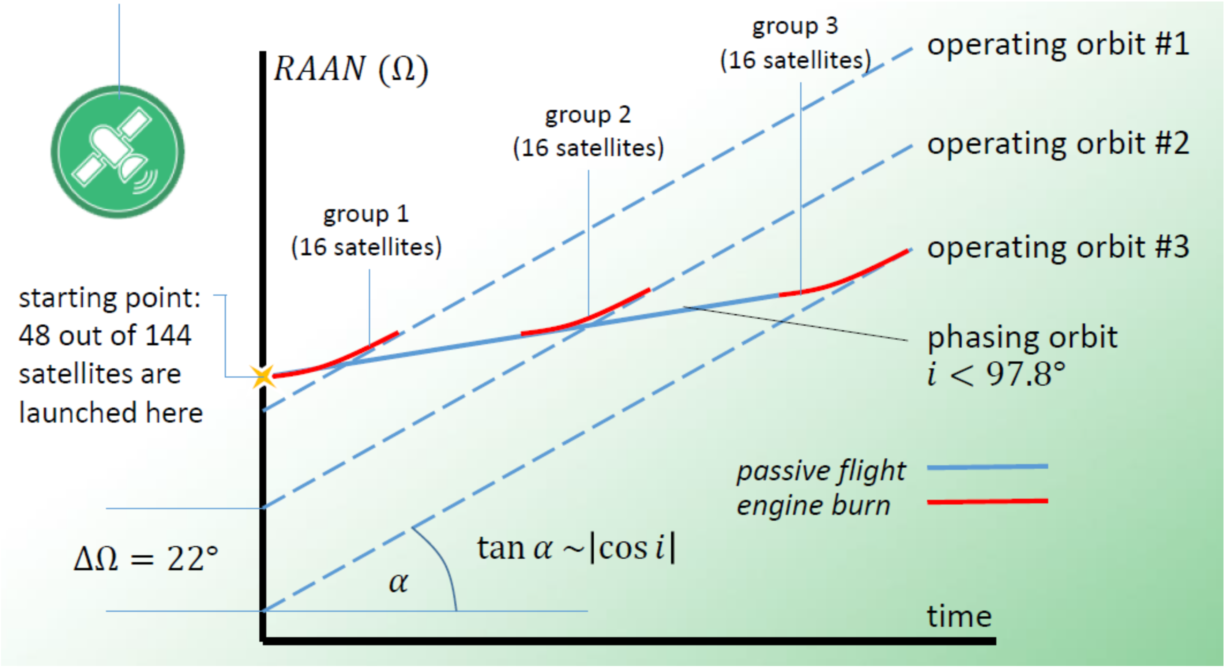

Figure 4. Non-coplanar orbit phasing strategy.

According to this scheme from Ref. 4, a modelling was conducted for a number of satellites launched to one point but destined for different RAANs. The RAAN over time for three such satellites is shown in Fig. 5.

For 700 kg satellites, the amount of propellant used here is about 15 kg. We can of course vary the inclination difference to save more propellant, but this will also prolong the overall time consumed by the maneuvers.

It is also technically possible to do the same with chemical propulsion, and that would be faster due to the higher thrust it provides, but the mass consumed (up to ¼ of initial spacecraft mass) makes this strategy questionable, more so considering that the station-keeping and deorbiting might then consume the same mass on top of it.

Table 1 shows how the parameters differ when phasing a constellation of 700 kg satellites into three planes, with the RAAN difference between neighboring planes of 22.25°. It shows thrust efficiency, propellant consumption, and time spent to reach the operating orbit by the second and the third spacecraft. The parameters were compared for the GT ion thruster developed by Avant-Space Systems, SPT Hall thrusters and chemical thrusters typically used in modern upper stages.

It is worth mentioning that the problem of such phasing is not trivial, and to this moment

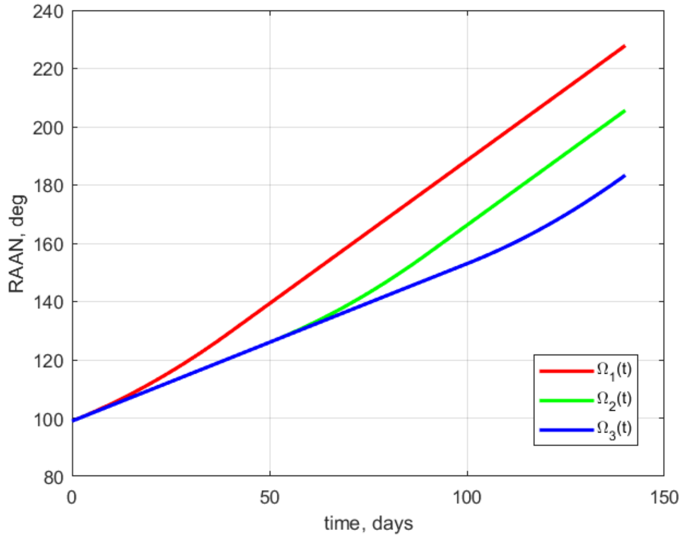

Figure 5. RAAN evolution for three satellites maneuvering to their positions.

no constellations were launched where this strategy would be applied. Nevertheless, at the same time, satellite manufacturers concede that in the nearest future non-coplanar orbit transfer will be more common, and those

Table 1. Maneuvers parameters for different propulsion systems.

	Thrust efficiency, W/mN	Propellant mass, kg	Time, 2nd plane, days	Time, 3rd plane, days
GT	25	15	105	158
SPT	18	35	90	140
Chemical	0	132	49	99

designing constellations now consider it more. The spacecraft energy efficiency of 5 W/kg used in the models is an optimistic estimate of the future spacecraft power capabilities. If we instead consider the energy efficiency of modern spacecraft that were not designed for supporting power consuming payload of performing such maneuvers with electric propulsion, then the non-coplanar phasing problem with satisfactory maneuver times cannot be solved at all.

It is worth mentioning that the problem of such phasing is not trivial, and to this moment no constellations were launched where this strategy would be applied. Nevertheless, at the same time, satellite manufacturers concede that in the nearest future non-coplanar orbit transfer will be more common, and those designing constellations now consider it more. The spacecraft energy efficiency of 5 W/kg used in the models is an optimistic estimate of the future spacecraft power capabilities. If we instead consider the energy efficiency of modern spacecraft that were not designed for supporting power consuming payload of performing such maneuvers with electric propulsion, then the non-coplanar phasing problem with satisfactory maneuver times cannot be solved at all.

D. Assessment summary

The calculations show that, generally speaking, for the spacecraft with relatively low area to mass ratio, using electric propulsion for station-keeping is not critical. Only for the low altitudes such as 500 km, where all-chemical mission can blow up to 10% of the initial satellite mass for station-keeping in 10 years it might be feasible to use high impulse thruster, such as ion thruster, that will consume 1% instead. But even in this case other factors also come to play when considering the architecture of a possible missions:

1. Cost-efficiency: it might be more feasible to launch additional 5 kg of propellant than to buy an expensive ion thruster;
2. Constructive complexity: the mass saved by the high impulse might be negated by big-sized subsystems of an ion thruster (control unit, RF-generator, etc.);
3. Reliability (redundancy is more possible with constructively simple chemical thrusters).

When talking about deorbiting, on the contrary, the higher the altitude, the clearer it is that a thruster with higher specific impulse is needed. If chemical propulsion is used, deorbiting can consume 10 to 15 percent of the total spacecraft mass.

The analysis conducted shows a possible range of the thruster parameters that is suitable for possible future spacecraft. These parameters are shown in Table 2.

Table 2. Requirement ranges of the thruster parameters.

SC mass, kg	Maneuvers	Power, W	Thrust, mN	Isp, sec
< 150	Station-keeping	< 300	< 12	> 1000
< 150	Deorbiting	< 300	< 12	> 1500
< 800	Station-keeping	< 1000	< 60	> 1000
< 800	Deorbiting	< 1000	< 60	> 1500
< 800	In-orbit and non-coplanar phasing	< 3000	< 120	> 3000

III. Experimental Analysis

A. Experimental setup and measurement procedure

In this work, a stainless steel vacuum chamber was used, 800 mm wide, 800 mm high and 750 mm deep. The air was pumped out by Korea Vacuum Limited DRP-1300 fore pump and KYKY TCDP-11 turbomolecular pump.

A schematic of the laboratory model of the ion thruster is shown in Fig. 6.

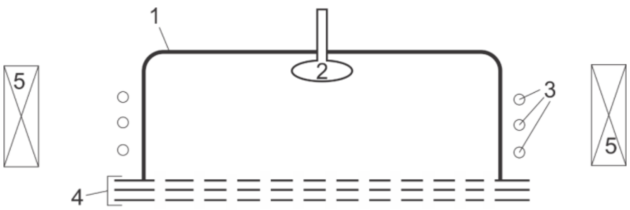

Figure 6. Ion thruster scheme.
1 – quartz discharge chamber, 2 – gas distributor, 3 – solenoidal antenna, 4 – ion-optical system, 5 – electromagnet.

The ion thruster consists of a discharge chamber, a gas distributor, a radio-frequency power input unit, an ion-optical system (which itself consists of three perforated electrodes), and a magnetic system.

The RF power input unit is a triple-coil solenoidal antenna, located on the side surface of the discharge chamber. The antenna is made of a copper tube with a diameter of 3 mm.

The ion-optical system (IOS) consists of three perforated electrodes (emitting, accelerating and decelerating) with 60% transparency,

The magnetic system consists of one or two electromagnets. The magnets create a longitudinal magnetic field in the discharge chamber.

The way the ion thruster is mounted in the vacuum chamber is illustrated in Fig. 7.

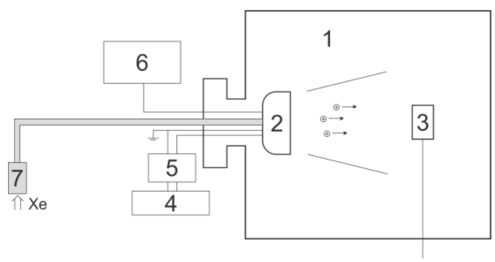

Figure 7. Experimental setup scheme.
1 – vacuum chamber, 2 – ion thruster laboratory model, 3 – energy analyser, 4 – RF power source, 5 – matching box, 6 – DC power supply for ion-optical system, 7 – ball-type flowmeter.

For ignition and maintaining the discharge in the thruster, antenna clips are connected to the RF generator through the matching box. The setup is equipped with Advanced Energy radio-frequency generators with frequencies of 2, 4 and 13.56 MHz. Power output may be 0-1000 W.

The automatic matching system consists of two variable vacuum capacitors and an inductor. In the whole range of discharge parameters, the matching system used was able to produce the reflected power of less than 10% of the forward power.

To produce an ion beam the voltage is applied on the electrodes of the ion-optical system, according to an “acceleration-deceleration” pattern. Powering up the electrodes is done with PSPLASMA SDC1521D5PR and SDC102D1R power supply units.

Filling the thruster with propellant (Xenon) was done with the Celerity FC-280SAV flowmeter.

The experiments were conducted with the xenon flow of 3-10 sccm, with the pressure in the vacuum chamber no more than 4·10-4 Torr. External magnetic field density was in range of 0-50 Gs. The lengths of discharge chambers in the test were 3, 4, 5, 7, and 10 cm.

The experiments were conducted under the following pattern:

1. Xenon was injected into the thruster model, and the discharge ignited;
2. +1000 V potential was applied to the emitting electrode of the IOS, the accelerating electrode potential was chosen to minimize the leakage current;
3. A dependency was measured between the ion beam current and the RF generator power.

The methods used to measure the power coupled to plasma are described in Ref.5.

With the measured values of *Pgen, Ppl* and the ion beam current *ib*, two values of ion “cost” were acquired, *Ci* and *Ci**, as show Eq.3 and Eq.4 below.

$$C_i = P_{gen}/i_b \tag{3}$$

$$C_i^* = P_{pl}/i_b \tag{4}$$

B. Test results

First, the results of optimizing the discharge in the thruster model with inductive discharge with no magnetic field will be discussed. Then, how the thruster parameters change after applying the external magnetic field will be studied.

Figure 8 shows the measured RF generator power needed for acquisition of the given ion beam current versus the xenon flow.

One can see that the graphs are quite similar to those acquired in Ref. 6. When the flow is high, the power P_{gen} needed for acquisition of the specific i_b weakly depends on the xenon flow. On the other hand, with less flow, the values of P_{gen} raise steeply.

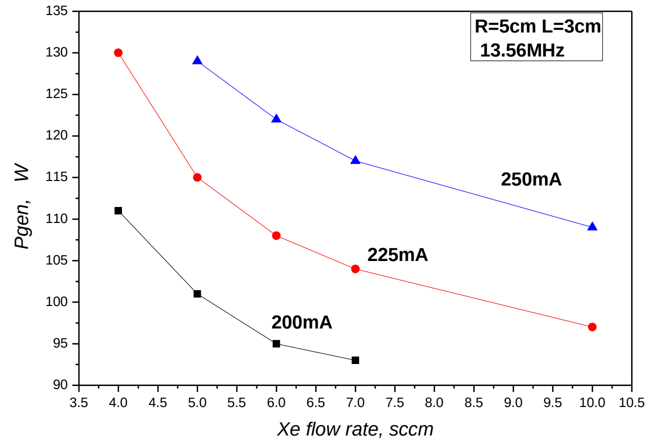

Figure 8. RF generator power needed for acquisition of the given ion beam current versus the xenon flow.

The experiments show that the values of P_{gen} needed for the required ion beam current depend heavily on the discharge chamber length and the generator's operating frequency. Figure 9 shows the ion current i_b obtained from the thruster model, and the $Ci = P_{gen} / i_b$, versus the length of the discharge chamber. The modes chosen for comparison correspond to the flow of 4 and 5 sccm and the power of 110 W. This power P_{gen} is close to the operating point of the RIT-10 thruster Ref. 7. The flow of 4 sccm that is chosen is slightly less than that of the RIT-10.

However, when analysing the results one must consider that there tests were conducted in a discharge chamber of a smaller size, and while evaluating the thruster's parameters the reverse flow of atoms through the holes in the IOS from the vacuum chamber to the discharge chamber was not taken into account. It is also worth mentioning that while working with a discharge chamber of the length less than 5 cm and frequencies less than 13.56 MHz, there were difficulties encountered in the ignition and supporting a stable discharge. In this manner, a stable discharge with operating frequencies of 2 and 4 MHz and with corresponding discharge chamber lengths less than 7 and 4 cm has not been achieved.

Before moving to the obtained results, it is worth mentioning the dependency of the efficiency of RF power coupling to plasma shown in Fig. 10. It can be seen that, given the conditions of the experiments, just above half of the power generated was consumed by the plasma, and the rest was dissipated in external circuit. It is notable that the values of P_{pl}/P_{gen} weakly depend on the chamber length and generator power. The latter indicates that when the operating frequency changes, the losses in the external current raise proportionally to the equivalent resistance of the plasma.

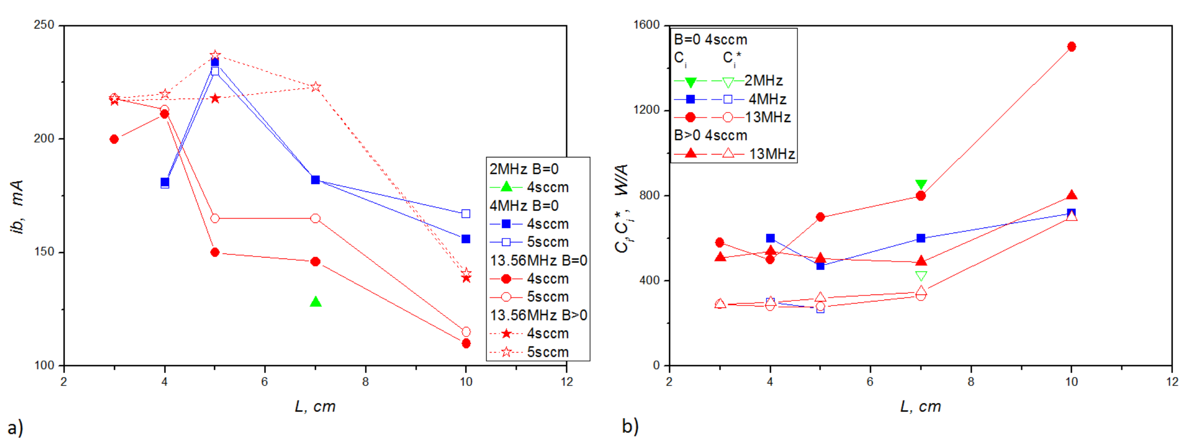

Figure 9. Ion beam current (a) and ion cost (b) obtained with xenon flow of 4 sccm and the generator power of 110 W with different length of discharge chamber.

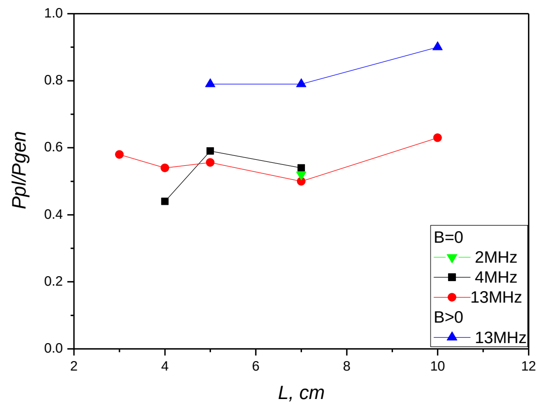

Figure 10. Efficiency of the radio-frequency power coupling to plasma vs the length of the discharge chamber. Xenon, 4 sccm, P_{gen} = 110W.

The results obtained have shown strong dependency between the ion beam current, and the discharge chamber length and the operating frequency of the generator. The former result is no surprise. The rising of ion cost in a discharge chamber of a less-than-optimal length is due to the reduced lifetime of the neutral particles in the discharge chamber. If the chamber length is more than the optimal, the ion current falls, because it is required here to create a dense plasma in a big volume. The second result showing a strong dependency between ib and the generator frequency indicates the significant role of the capacitive component in maintaining the discharge in the chamber.

The best result of the thruster modes without the external magnetic field was obtained operating at the frequency of 4 MHz in the chamber 5 cm long. The values of the ion cost achieved ion cost were close to those distinctive to the RIT-10 [7]. However, one should not forget that given the experimental conditions a significant part of the power was dissipated in external circuit. Figure 9 (b) shows the ion cost C_i*, calculated basing on the power deposited into plasma, $C_i^* = P_{pl} / i_b$. Comparing C_i and C_i* indicates that there is a way to improve the thruster parameters significantly by increasing the percentage of the power consumed by the plasma. It is clear that in order to achieve energy-efficient thruster operation modes it is essential that, firstly, the power loss in the external current (and so Rant) is minimized, and, secondly, that the discharge process is so organized that the equivalent resistance of the plasma R_{pl} would be maximized. The latter can be achieved by putting the discharge chamber into an external magnetic field with the density corresponding to the condition of resonant coupling of RF power. Figure 11 shows the ion current obtained depending on external magnetic field density.

It is seen that at 4 Mhz the ion current raises only insignificantly with changing of the B. At the same time, at 13.56 MHz the i_b raises significantly. The magnetic field density range where the raising ion beam current can be seen lies between the electron-cyclotron resonance (ECR) point, and the “helicon land”. The paper [8] shows theoretically that plasma density growth leads to shifting the ECR point to the bigger Bs, and the same is obtained in the discussed experiments.

One of the reasons why the ion beam current raises is better deposition of the RF power into plasma, which is clearly seen in Fig. 10. Applying magnetic field to the discharge leads to not only the raising ion current and decreasing ion cost, but also to changing the dependency between i_b and L, which becomes smoother.

Thusly, the experiment results show that key factors influencing the thruster parameters are the length of the discharge chamber, operating frequency and the density of the external magnetic field. At the operating frequency of 2 MHz and using a triple-coil solenoidal antenna, the operating modes lean towards the generator power unavailable in the most LEO spacecraft. The frequency of 4 MHz allows obtaining the best result in a discharge mode without external magnetic field. Applying the magnetic field while operating at higher frequencies leads to better consumption of the RF power, less ion cost, and wider range of possible discharge chamber lengths.

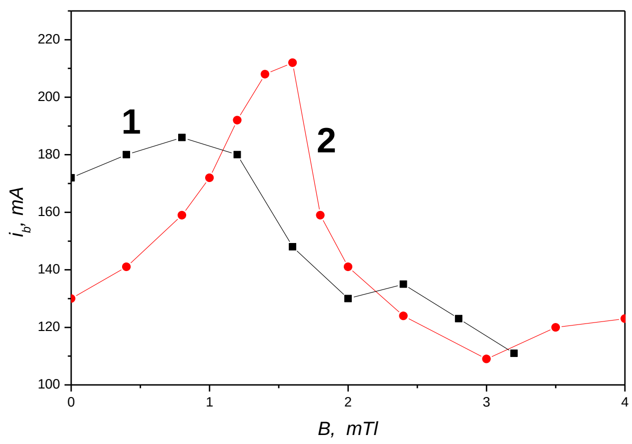

Figure 11. Ion current vs external magnetic field density. 1 – 4 MHz, L = 10 cm, 5 sccm, 120 W; 2 – 13.56 MHz, L = 5 cm, 4sccm, 110 W.

IV. Conclusions

This paper describes an assessment of possible applications of an ion thruster using an external magnetic field allowing optimizing the power coupling to plasma and raising plasma density at given RF power values. The experiments show that the ion cost of about 450 W/A can be achieved. Depending on the voltage applied to the grid (and thus on the specific impulse) this can mean that the thruster can work consuming as low as 25-30 watts per 1 mN of thrust (with I_{sp} of about 1500 sec). It is possible to increase the I_{sp} applying higher voltage to the grids, but the thrust efficiency might be slightly higher this way. The study conducted on the possible applications of the thruster in various space missions show that a thruster with such parameters is highly applicable for station-keeping and deorbiting of spacecraft and will be anticipated on the market.

References

[1]Mazouffre, S., "Electric propulsion for satellites and spacecraft: established technologies and novel approaches", *Plasma Sources Sci. Technol*. 25 (2016) 033002 (27pp).

[2]Loeb, H.W., "Radio Frequency Ion Sources for Electrostatic Propulsion (Hollow Cathode Design for Electron Bombardment Radio Frequency Ion Thruster Source)", *Proceedings of the Symposium on Ion Sources and Formation of Ion Beams*, 1971, pp. 77-84

[3]Kolobov, V.I., Godyak, V.A., "Inductively coupled plasmas at low driving frequencies", *Plasma Sources Sci. Technol.* 26 (2017) 075013 (13pp).

[4]Kharlan, A., Ruchenkov, V., Teplyakov, V., "Mobile Satellite Communication System Based on New Digital Phased Array Beamforming Technology", *Proceedings of the 66th International Astronautical Congress, Jerusalem, Israel*, 2015, IAC-15,B2,1,4,x31299

[5]Alexandrov, A.F., Kralkina, E.A. et al., "ON THE POSSIBILITIES OF RF ION THRUSTERS OPTIMIZATION*", IEPC-2005-122*.

[6]Lenz B., Schweitzer M. and Loeb H.W., "Improved RF-Coupling Method for RIT-Engines", *AIAA Journal*, 79-2057, 1979

[7]Goebel, D.M., Katz, I., "Fundamentals of Electric Propulsion: Ion and Hall Thrusters" *JPL Space Science and Technology Series*, Wiley, 2008, pp. 148-158.

[8]Vavilin K.V., Plaksin V. Yu., Ri Kh.M. Rukhadze A.A., "Low power RF power sources for technological applications. II. Plasma sources under anomalous skin-effect conditions", *Technical physics*, 49, N6, 2004, pp. 686-690.